Indirectly Driven, High Convergence Inertial Confinement Fusion Implosions

M. D. Cable, S. P. Hatchett, J. A. Caird, J. D. Kilkenny, H. N. Kornblum, S. M. Lane, C. Laumann, R. A. Lerche, T. J. Murphy, J. Murray, M. B. Nelson, D. W. Phillion, H. Powell, and D. B. Ress

Lawrence Livermore National Laboratory, P.O. Box 808, Livermore, California 94551

(Received 23 May 1994)

A series of high convergence, indirectly driven implosions has been done with the Nova Laser Fusion facility. These implosions were well characterized by a variety of measurements; computer models are in good agreement. The imploded fuel areal density was measured using a technique based on secondary neutron spectroscopy. At capsule convergences of 24:1, comparable to what is required for the hot spot of ignition scale capsules, these capsules achieved fuel densities of 19 g/cm^3. Independent measurements of density, burn duration, and ion temperature gave $n\tau\theta = 1.7 \pm 0.9 \times 10^{14}$ keV s/cm^3.

PACS numbers: 52.70.Nc, 28.52.Av, 28.52.Cx, 52.55.Pi

High grain inertial confinement fusion will most readily be achieved with hot spot ignition [1,2] where a relatively small mass of gaseous fuel at the center of the target is heated to 5–10 keV, igniting a larger surrounding mass of fuel at higher density but lower temperature. Existing lasers are too low in energy to achieve thermonuclear gain, however, hydrodynamically equivalent implosions can demonstrate that the important, scalable parameters of ignition capsules are scientifically and technologically achievable. The experiments described in this Letter, utilized gas-filled glass shells that were driven symmetrically by x rays produced in a surrounding cavity (*Hohlraum*). These implosions achieved high convergence ratios (initial capsule radius/final fuel radius) in the range required for ignition scale capsules and produced an imploded configuration (high density glass with hot gas fill) that is equivalent to the hot spot configuration of an ignition scale capsule. Other recent laser driven implosions [3,4] have achieved high shell density but at lower convergences and without a well-defined hot spot. Also other experiments [5,6] have used very low density gas fill to reach high convergence with unshaped drive (see below) which results in a relatively low shell density. Moreover, unlike previous experiments, even at the highest convergence ratios the implosions described here had neutron yields averaging 8% of that calculated for an idealized, clean, spherically symmetric implosion (see below). The implosions were modeled, with the inclusion of nonideal effects, with detailed computer codes such as LASNEX [7], a coupled radiation transport, hydrodynamics, and Monte Carlo burn particle transport code. All observable quantities were in close agreement with these simulations, demonstrating good understanding of the implosions.

The targets were indirectly driven gas filled microballoons as shown in Fig. 1. A relatively small capsule (diameter of 16% of the *Hohlraum*) was chosen to allow the use of secondary neutrons for the determination of fuel areal density (see below). Equimolar deuterium/tritium or deuterium filled glass capsules were used. Capsule fill pressures were varied from 25–200 atm which changed the level of capsule convergence for constant drive. Ten Nova beams (2.1 kJ each at 0.35 μm) were incident on the interior of a uranium *Hohlraum* at 2×10^{15} W/cm^2 and produced an x-ray flux on the surface of the capsule; the *Hohlraum* geometry is also shown in Fig. 1. Measured laser pulse shape and corresponding brightness temperature of the x-ray drive $T_{\rm rad}(t)$ are shown in Fig. 2. X-ray drive was measured using a multichannel, K- and L-edge filtered, x-ray spectrometer looking into the *Hohlraum* at both directly illuminated laser spots and an indirectly illuminated wall [8]; observed spectra were nearly Planckian. The x-ray drive versus time dependence was chosen to optimize the pressure-density trajectory of the capsule compression as much as possible consistent with hydrodynamic instability limitations [9]. Use of a glass shell and uranium *Hohlraum* minimizes the x-ray preheating of the capsule. The capsule implosion is driven by pressure generated by ablation of the outer surface material. Under the conditions of these experiments (x-ray brightness temperature is sufficiently low so the ablation front is subsonic, time scale is sufficiently short so the ablated material is optically thin to the driving x rays) it can be shown [10] that the ablation pressure is approximately given by $P_{\rm abl} = 0.5\,\sigma T_{\rm rad}^4/(RT_{\rm rad}/\mu)^{1/2}$, where σ is the Stefan-Boltzmann constant, R is the gas constant, and μ is the molecular weight. This gives 8 Mbar at the foot

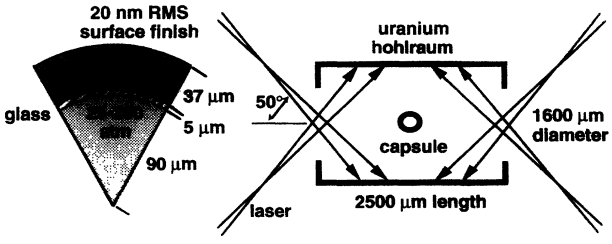

FIG. 1. Diagram of capsule and indirect drive *Hohlraum* geometry.

 0031-9007/94/73(17)/2316(4)$06.00

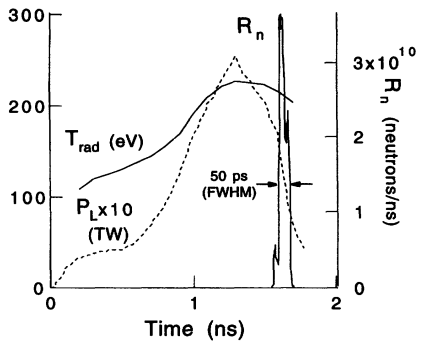

FIG. 2. Observed laser power (P_L), *Hohlraum* temperature (T_{rad}) and neutron reaction rate (R_n) for 100 atm DT filled capsules.

of the pulse (t = 0.2 ns) and 110 Mbar at the peak of the pulse (t = 1.4 ns).

Convergence of these capsules is limited by the x-ray drive symmetry. The *Hohlraum* does not produce a perfectly uniform drive distribution, but any position on the capsule "sees" an integral over the various elements of the *Hohlraum* (directly illuminated wall regions, indirectly illuminated regions and entrance holes), so higher moments of the drive distribution are strongly smoothed. (Typically, the drive symmetry is analyzed in terms of spherical harmonics which reduce to Legendre polynomials with cylindrical symmetry.) The remaining systematic asymmetry is controlled by choosing the relative values of capsule radius, *Hohlraum* dimensions, and the first bounce position of the laser beams along the *Hohlraum* wall to minimize the $P_{2,4}$ effects. $P_{1,3}$ effects are eliminated by symmetry. Some lower moment asymmetry remains, which is time dependent, because both the albedo of the wall and the effective positions of the laser spots change as hot wall material moves into the *Hohlraum*. By design, simulations with the configuration used in these experiments show a P_2 asymmetry that changes sign, is at most 8%, and averages to a very low value. Details of *Hohlraum* design are being reported elsewhere [11].

A second source of time-dependent drive asymmetry is random variations due to imprecise laser beam-to-beam power balance and pointing. This is minimized by precise control of the laser. We maintain tolerances of 8% (rms) beam-to-beam power balance during the foot of the laser pulse and 4% power balance during the peak. Pointing tolerance is $\pm 30\mu$m (rms). This control gives a power balance on the capsule that from simulations is uniform to 2% (rms) at peak power and 4% in the foot. Early experiments demonstrated that this level of power balance is a necessary requirement for high convergence.

Burn averaged fuel density and capsule convergence were determined from measurement of fuel areal density, "ρR" $\equiv \int_{\text{fuel}} \rho(r)dr$. If ρ is assumed to be uniform then $\rho = \rho_0(\rho R/\rho_0 R_0)^{3/2}$, so a determination of ρR gives both ρ and R. ρR was measured by the secondary neutron technique [12–16]. This technique relies upon the observation of 12–17 MeV "secondary neutrons" produced via the D(T,n)^{4}He reaction in an initially pure deuterium fuel. The 1.01 MeV tritons are produced in the primary fusion reaction D(D,p)T. If the tritons do not slow significantly as they traverse the fuel, then the fraction of tritons producing secondary neutrons is proportional to fuel ρR. For the fuel conditions in this work (low temperature with mixed pusher material, see below), ρR values above a few mg/cm^2 cause significantly triton slowing, and corrections must be made for the cross-section energy dependence. Cable and Hatchett [12] have outlined how this can be done based on a measurement of the secondary neutron energy spectrum. Since the cross section rises with decreasing triton energy, this correction typically results in a ρR value that is lower than that calculated for the case of little slowing. The secondary neutron energy spectrum was measured with an array of neutron time-of-flight detectors [17]. A spectrum obtained by summing all the 25 atm capsule data (10 implosions) is shown in Fig. 3; also shown is the simulated spectrum discussed further below.

Primary neutron yield [18] was determined by activation measurements of In samples placed near the target, and pusher areal density [19] was measured by determining the amount of neutron-induced activation of Rb dopants in the glass shell. Burn duration and burn time relative to the start of the laser pulse were determined with a scintillator-streak camera arrangement [20] capable of measuring neutron production as a function of time with 20 ps resolution, Figure 1 shows an example of the measured reaction rate. Fuel ion temperature was measured by observing the temperature dependent Doppler broadening of the primary neutron energy spectrum with a neutron time-of-flight system [21] that was simpler and separate from that used for secondary neutron spectroscopy.

Observed fuel areal densities up to 16 mg/cm^2 allowed determination of the densities and convergences plotted

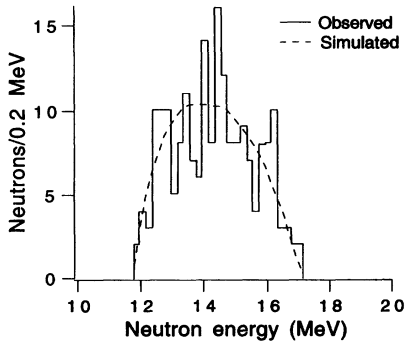

FIG. 3. Secondary neutron energy spectrum. Measured with array of neutron time-of-flight detectors. Observed is sum of all 25 atm capsules.

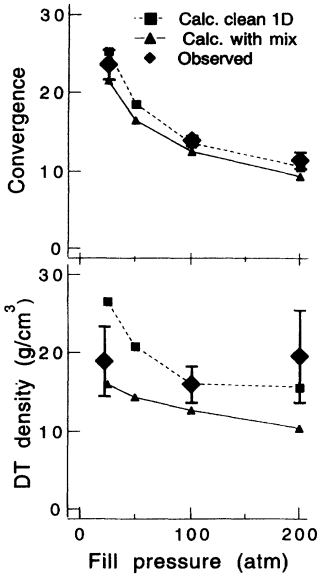

FIG. 4. Observed and calculated convergence and density as functions of capsule fill pressure. Density is expressed as equivalent deuterium/tritium fill even when capsule is deuterium filled.

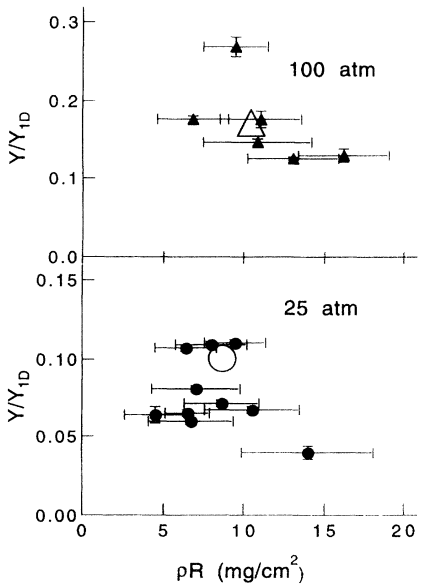

FIG. 5. Observed neutron yields and ρR values. Large open symbols are from simulations which include mix. Yields are plotted as a fraction of simulated clean 1D yield.

in Fig. 4. For this figure, experimentally observed values were averaged over several implosions (2 at 200 atm, 6 at 100 atm, and 10 at 25 atm), and the errors were dominated by the statistical sample size of observed secondary neutrons. It can be seen in Fig. 4 that the observed values are consistent with or better than those expected from simulations if the effects of fuel-pusher mixing are included at the level which current models [9] predict given the capsules' surface finish. (The calculations labeled clean 1D include no mix effects and assume perfect spherical symmetry; this is physical unrealistic since the fuel/glass interface is Rayleigh-Taylor unstable near peak compression but is commonly quoted as an "ideal" limit.) Fuel-pusher mixing introduces two important effects; mixing of high-Z matter into the fuel enhances the triton slowing, and mixing of fuel outward into the pusher decreases the fuel convergence. Secondary neutron spectroscopy allows us to quantify these effects since the secondary neutron energy spectrum is dependent upon the level of the triton slowing. It can be seen in Fig. 3 that the simulation gives good agreement with the observed spectrum which further supports the validity of the mix modeling.

Primary neutron yields for these implosions were 2×10^7 to 1.4×10^8 with pure deuterium fill (2.45 MeV neutrons) and were 3×10^8 to 3×10^9 with 50/50 deuterium/tritium fill (14 MeV neutrons) with the lower yields observed for the higher convergence, lower fill capsules. Figure 5 shows the individual capsule yields and ρR values compared to both clean 1D and mixed simulations. ρR scatter is consistent with the measurement error, but yield scatter is larger since yield is very sensitive to the fuel ion temperature (roughly proportional to T^5 for this temperature range), and the fuel temperature is affected by small variations in capsule surface finish, capsule dimensions, and laser energy. (If the glass pusher were replaced with a layer of cryogenic liquid DT, as it is in most current ignition scale capsule designs, then the yield would be much less sensitive to mix.) Fuel ion temperatures were 0.9 ± 0.4 keV for all cases; at this temperature the observed fuel density corresponds to a final fuel pressure of 16 Gbar. Glass shell ρR was observed to be 73 ± 16 mg/cm^2 (100 atm) and 60 ± 19 mg/cm^2 (25 atm) in a pair of shots at each fill. This compares with the simulated values of 54 and 81 mg/cm^2, respectively. In the 25 atm simulations, the peak burn-time glass density is 160 g/cm^3. Burn duration for the 100 atm capsules was measured to be 50 ± 15 ps and occurred at 1600 ± 100 ps after the start of the laser pulse (see Fig. 2); simulations gave 33 ps and 1603 ps, respectively. From simulations and measurements, shock breakout from the inner shell surface, which corresponds to initial fuel movement, does not occur until 1 ns after the start of the laser pulse. This gives an average implosion velocity of 1.4×10^7 cm/s; simulations show that peak velocity is 1.8×10^7 cm/s. Using the observed fuel density and burn duration, a confinement parameter of $n\tau = 1.9 \pm 0.6 \times 10^{14}$ s/cm^3 is obtained.

These experiments, which utilized better diagnostic techniques than previous work allowed detailed comparisons to simulations and permitted a deeper understanding

of the sensitivity of the implosion process to factors such as laser power balance. These implosions have provided an integrated test of our ability to control and model the implosion dynamics sufficiently so as to achieve convergence levels comparable to those required for the hot spot of an ignition scale capsule.

This work was performed under the auspices of the U.S. DOE by Lawrence Livermore National Laboratory under Contract No. W-7405-Eng-48.

[1] J. Nuckolls *et al.,* Nature (London) **239**, 139 (1972).
[2] J. D. Lindl, R. L. McCrory, and E. M. Campbell, Phys. Today **45**, No. 9, 32 (1992).
[3] F. J. Marshall *et al.,* Phys. Rev. A **40**, 2547 (1989).
[4] H. Azechi *et al.,* Laser Part. Beams **9**, 193 (1991).
[5] J. D. Kilkenny *et al., Plasma Physics and Controlled Nuclear Fusion Research* (International Atomic Energy Agency, Vienna, 1989), Vol. 3, p. 29.
[6] H. Nishimura *et al., Plasma Physics and Controlled Nuclear Fusion Research 1992* (International Atomic Energy Agency, Vienna, 1993), Vol. 3, p. 97.
[7] G. B. Zimmerman and W. L. Kruer, Comments Plasma Phys. Controlled Fusion **11**, 51 (1975).
[8] H. N. Kornblum, R. L. Kauffman, and J. A. Smith, Rev. Sci. Instrum. **57**, 2179 (1986).
[9] S. Haan, Phys. Rev. A **39**, 5812 (1989).
[10] S. P. Hatchett, Lawrence Livermore National Laboratory, Report No. UCRL-JC-108348, 1991.
[11] L. Suter *et al.,* Phys. Rev. Lett. **73**, 2328 (1994).
[12] M. D. Cable and S. P. Hatchett, J. Appl. Phys. **62**, 2223 (1987).
[13] E. G. Gamalii *et al.,* JETP Lett **21**, 70 (1975).
[14] T. E. Blue and D. B. Harris, Nucl. Sci. Eng. **77**, 463 (1981).
[15] H. Azechi *et al.,* Appl. Phys. Lett. **49**, 555 (1986).
[16] M. D. Cable *et al.,* Bull. Am. Phys. Soc. **31**, 1461 (1986).
[17] M. B. Nelson and M. D. Cable, Rev. Sci. Instrum. **63**, 4874 (1992).
[18] S. M. Lane *et al.,* Lawrence Livermore National Laboratory, Report No. UCRL 50021-86, 1986.
[19] S. M. Lane and M. B. Nelson, Rev. Sci. Instrum. **61**, 3298 (1990).
[20] R. A. Lerche, D. W. Phillion, and G. L. Tietbohl, in Proceedings of SPIE 2002, edited by P. W. Roehrenbech (SPIE, International Society for Optical Engineering, Bellingham, WA, 1993), p. 153.
[21] T. J. Murphy and R. A. Lerche, Rev. Sci. Instrum. **63**, 4883 (1992).

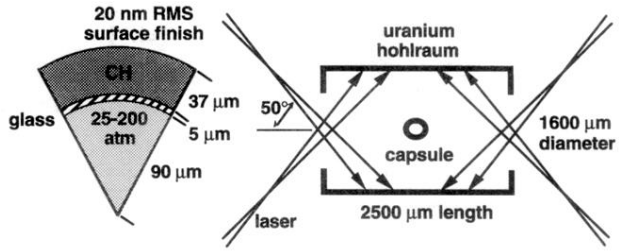

FIG. 1. Diagram of capsule and indirect drive *Hohlraum* geometry.